IN VITRO AND IN VIVO EXPERIMENT OF ANTIBACTERIAL SILVER NANOPARTICLE-FUNCTIONALIZED BONE GRAFTING REPLACEMENTS

By

ATHEENA MILAGI PANDIAN S. * RASHIKA MURUGAN ** MOHAMMED SAHIL S. ***

*-*** *Atheenapandian Private Limited, Chennai, Tamil Nadu, India.*

https://doi.org/10.26634/jms.12.1.20892

Date Received: 17/06/2024 *Date Revised: 26/06/2024* *Date Accepted: 08/07/2024*

ABSTRACT

Infection is a serious risk in transplant surgery and should be carefully considered while developing biomaterials. Silver nanoparticles (AgNPs) are gaining popularity due to their ability to enhance antibacterial capabilities against a wide range of bacterial types. This study sought to create two antibacterial bone regenerations by incorporating AgNPs into bovine bone particles (BBX) (Product 1) and a light cross-linked hydrogel GelMA (Product 2). Scanning electron microscopy was used to characterize the constructions. PrestoBlue™ was used to assess osteoblast and osteoclast metabolic activities on the creations. Optimized AgNP functionalized BBX and GelMA were tested in a rabbit cranial 6mm defect model to assess their regeneration ability. The presence of AgNPs appears to increase. In vitro, osteoblasts proliferated more than AgNP-free controls. It is found that a 100 µg dosage of AgNPs effectively suppresses bacteria while minimizing negative effects on bone cells. The rabbit model indicated that both BBX and GelMA hydrogels loaded with AgNPs were biocompatible, with no evidence of necrosis or inflammation. Grafts functionalized with AgNPs can defend against germs while also serving as a platform for bone cell adhesion.

Keywords: In Vitro, In Vivo, Bone Grafting, AgNPs, Biocompatible, Silver Nanoparticles, Replacements, Bone Particles.

INTRODUCTION

In dentistry, newly regenerated bone tissue of sufficient volume is required to restore maxillofacial esthetics and musculoskeletal functioning. The extent of a bone defect has a significant impact on its ability to heal itself. A critical-sized defect is caused by injury, malignancy, inflammation, disease, or tooth extraction that does not heal spontaneously. Such defects necessitate bone grafting, and bacterial infection might further impede the healing of the defect areas. Bacterial adhesion and biofilm formation have major effects, including bone graft failure, protracted hospitalization with antibiotic therapy, and, in many cases, several surgical operations that increase the patient's morbidity. Once established, biomaterials-associated infections are difficult to treat, even with high doses of antibiotics, they tend to keep going when the prosthetic device is removed, and systematic antibiotics might not be effective in eliminating such infections. The worldwide development of resistant bacteria to antibiotics has necessitated the employment of alternative infection-control measures (Abdelmoneim et al., 2022; Inchingolo et al., 2022; Cotton et al., 2019).

1. Methods

1.1 Silver Nanoparticles Preparation, Synthesis, and Characterization

Cotton et al. (2019) had detailed the manufacturing and

characterization of AgNPs. The amount of each substance was measured using inductively coupled plasma-mass spectrometry (ICP-MS, Agilent 7500CE apparatus, Agilent Technologies; California, USA). Images were taken utilizing a Philips CM100 BioTWIN TEM (Philips/FEI Corporation; Eindhoven, Holland) coupled with a LaB6 emitter and a MegaView III Olympus digital camera. The diameter of 100 particulates was determined manually using ImageJ software from the US National Institutes of Health in Bethesda, Maryland, USA (Porter et al., 2022).

1.2 GelMA Synthesis and Preparation

GelMA as a (5 wt%) was manufactured and produced as originally reported in this paper (Xu et al., 2019). To begin, jello was diluted in 10 wt% phosphatase-buffered saltwater (PBS). Then, 0.6 g of methacrylic anhydride per gram of collagen was added to the liquid and left to react for 1 hour at 50 °C with constant swirling. The solution was collected utilizing a 0.22 µm sterile filter, lyophilized under sterile conditions, and stored until needed (Porter et al., 2021).

1.3 Safety of OMB with AgNPs: Osteoblast Response

Bone was processed at temperatures of 100, 130, 160, and 190 °C for 2 hours to yield OMB granules. Granules measuring 1×2×2 mm were loaded with varying doses of AgNPs (0, 50, 100, and 150 µg/g) as described and dried. Granules with and without AgNPs were then put in 48-plate wells, with a minimum of 23 granules per well. The wells were supplemented with McCoy's media +15% fetal bovine serum (FBS) (200 µL), 100 µM L-ascorbic acid-2-phosphatase, 10 nM dexamethasone, and 5 mM β-glycerophosphate, and incubated for 16 hours at 37 °C with 5% CO2. The osteoblast cells (Saos-2 (ATCC® HTB-85™)) were seeded at 1.6 × 105 cells (Lim et al., 2019).

1.4 Scanning Electron Microscopy of the Final Constructs

Three specimens in each group were sputter deposited with a 10 nm gold-palladium layer (Emitech K575X, EM Technologies Ltd., Kent, England). Surfaces were studied at 30,000× magnification using a field-emission scan ray imaging (SEM) (Joel 6700F, Joel Ltd., Tokyo, Japan) in principal nuclear mapping mode employing a 10 kV acceleration voltage. Representative regions were discussed and contrasted (Martins & Rodrigues, 2020).

1.5 Animal Surgery

The study involved twelve mixed-gender Auckland white rabbits. The study shown in Figure 1 was carried out at Lund University in Sweden (Ethics number 5.8.18-02996/2020, sanctioned by the Malmö-Lund Animal Research Board). Three defects were treated with OMB, AgNP-OMB, and AgNP-GelMA-OMB, with one defect remaining untreated as a negative control (Figure 1). The animals were anesthetized using Ketamine (0.35 mg/kg) and Dexdomitor (0.1 mL/kg). Before surgery, the rabbits received a subcutaneous injection of carprofen 0.08mL/kg. The skull's hair was shaved, and the skin was iodine-treated and draped. The procedure was carried out using aseptic techniques and sterile tools. Lidocaine with adrenaline was injected around the surgical site. A linear incision was made from the nasal bone to the mid-sagittal (Porter et al., 2021).

2. Experimental Results

2.1 Silver Creation of Nanoparticle

The suspension of colloids of AgNPs appeared deep yellow/brown, indicating that the tiny particles remained stable and evenly distributed. The aerodynamic dimension of AgNPs, which was determined through DLS, was found to be 1–12 nm, with a concentration of 2510 µg/mL as assessed by ICP-MS. TEM scans revealed elliptical particles with a typical diameter of 5–6 nm (Porter et al., 2022; Xu et al., 2019).

2.2 Antibiotic Properties

The antibacterial property of OMB disks containing AgNPs

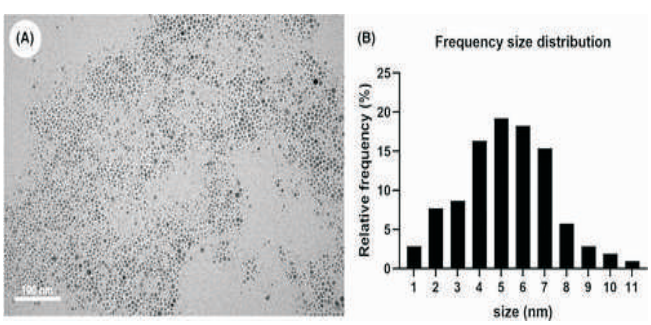

Figure 1. Schematic Diagram of Rabbit Skull Showing the Four Defects and Treatments

was evaluated using nutritional agar. Figure 2 shows the widths of the clear zone (inhibition zone) of bacterial inhibition after a 24-hour incubation of the agar plate at 37°C. The concentration of AgNP utilized in the constructions affected the inhibition zone diameters, which varied from 0.5 to 3 mm. With an increase in AgNP concentration, inhibition zones and, thus, antibacterial activity rose. As demonstrated in Figure 3, an inhibitory zone began to form at 75 µg/g and measured 0.5–1 mm for ***E. coli*** and 1.5–2 mm for ***S. aureus*** in the AgNP-bone disks containing 100 µg/g of AgNP (Abdelmoneim et al., 2023; Inchingolo et al., 2022; Mendes et al., 2022).

2.3 Metabolic Activity

Metabolic activity tests were performed on osteoblasts after 7 days. The 160°C bone continuously displayed increased metabolic activity and improved with increasing AgNP concentration, as shown in Figure 3. For the majority of constructions, the addition of AgNPs appears to increase metabolic activity when compared to controls without AgNPs. At 150 µg/mL of AgNPs, bone surfaces at 100, 130, and 190 °C showed increased variability and lower metabolic activity relative to those treated at 160 °C (Martins & Rodrigues, 2020). Increased AgNP concentrations did not affect osteoclast metabolic activity (Figure 4). In this study, BO appeared to promote osteoclast attachment, although all other treatments and controls shown comparable metabolic activity (Qing et al., 2018).

2.4 Surgical Results

No postoperative problems occurred, and all animals were killed at the appropriate time periods. Macroscopically, all defect areas were closed and filled with NB, as shown in Figure 4. At 4 weeks, bone defect locations grafted with OMB and AgNP-OMB showed visible graft particles embedded in newly produced hard tissue, while AgNP-GelMA-OMB appeared smooth. At 16 weeks, freshly produced bone tissue was homogeneous, with no significant clinical distinction of RG particles except for OMB, where particles were still visible. The AgNP-GelMA-OMB sites appeared darker than the other sites (Inchingolo et al., 2022).

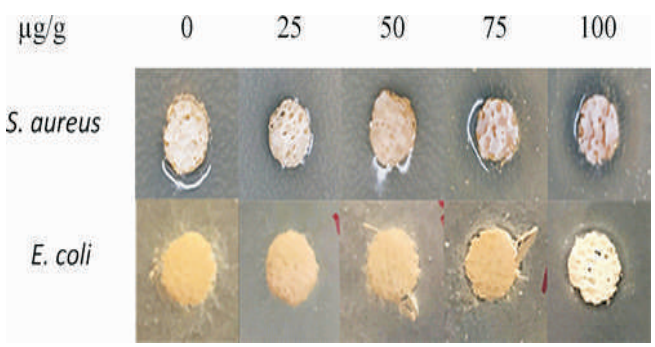

Figure 2. Representative Images of the Inhibition Zones of *E. coli* and *S. Aureus* as a Response to Increasing AgNP Concentration on the OMB Material (n = 3). Inhibitory Zones were Evident at AgNP Concentrations > 75 µg/g of Bone
Note: OMB, Optimized MoaBone

2.5 Histomorphometric Analysis

The quantification of NB, CT, and the remaining grafted nanoparticles showed no significant variance in CT or NB development between the test and control groups at 4 or 16 weeks, unlike 2D and 3D micro-CT studies. At 4 weeks, AgNP-OMB implanted defects contained considerably more grafting material than AgNP-GelMA-OMB. However,

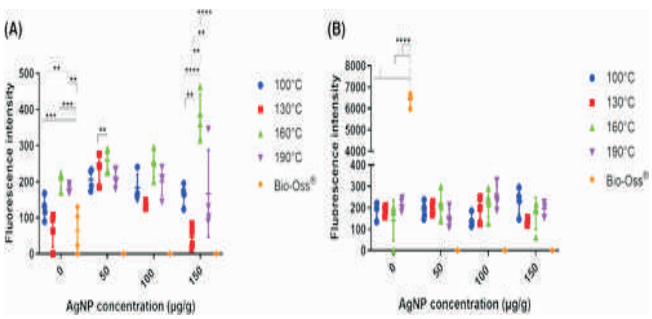

Figure 3. Macroscopic Healing of the Bone Defects and Empty Site at 4 and 16 Weeks of Healing (n = 6)Note: Red Circle Denotes the 6 mm Defect

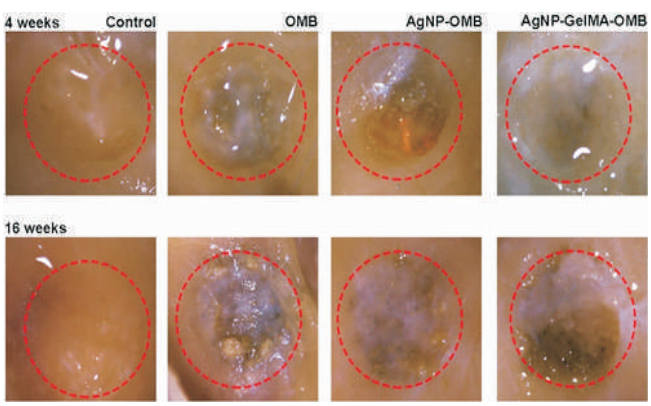

Figure 4. Macroscopic Healing of the Bone Defects and Empty Site at 4 and 16 Weeks of Healing (n = 6) Note: Red Circle Denotes the 6 mm Defect

there was no disparity in Na development at 16 weeks. There was no evidence that adding AgNP to OMB hampered bone healing when compared to OMB alone, nor that adding GelMA interfered with bone restoration when relative to OMB alone (Mukaratirwa-Muchanyereyi et al., 2022).

3. Results and Discussion

Designing innovative biomaterials with regenerative, antimicrobial, and low-toxicity qualities is critical to avoiding the common occurrences of microbial resistance and infection, which lead to the failure of oral and maxillofacial grafting surgeries. The use of AgNPs in biomaterials as a replacement for medicines provides antimicrobial properties in bone infection-prone locations, perhaps contributing to a reduction in the need for systemic antibiotics. This paper looked at the safety and regeneration properties of two AgNP-functionalized bone grafting materials. Product 1 was made from low-temperature deproteinized bovine bone (OMB), whereas Product 2 was a photocross-linked hydrogel (GelMA) that encased OMB (Wi & Patel, 2018). The two compounds were compatible with life, promoting the development of bones, and the addition of AgNPs had no detrimental effects in vivo. Considering the toxicity of the silver nanoparticles varies depending upon their quantity, shape, size, and the presence of a capping agent, drawing broad conclusions about biocompatibility is challenging. This paper used alpha lipoic acid-capped AgNPs, which are known to be antioxidants and anti-allergic and are known to minimize AgNP toxicity while still providing antibacterial protection (Abdellatif et al., 2022; Singh & Mijakovic, 2022).

Conclusion

This study demonstrated the successful incorporation of alpha-lipoic acid-encapsulated AgNPs as an antibacterial into new materials intended for bone restoration applications. A 100 µg/g dosage is safe for marrow cells and effectively inhibits bacterial growth. In vitro, incorporating alpha lipoic acid-capped AgNPs into the bone graft stimulated osteoblast growth, and there were no symptoms of resistance or adverse reactions in vivo. The two bone grafting materials disclosed, bone graft with nanosilver and bone graft with hydrogel with nanosilver, represent innovative therapeutic techniques that provide both protection from infections and bone regrowth.

References

[1]. Abdellatif, A. A., Alhathloul, S. S., Aljohani, A. S., Maswadeh, H., Abdallah, E. M., Hamid Musa, K., & El Hamd, M. A. (2022). Green synthesis of silver nanoparticles incorporated aromatherapies utilized for their antioxidant and antimicrobial activities against some clinical bacterial isolates. *Bioinorganic Chemistry and Applications*, 2022(1), 2432758.

https://doi.org/10.1155/2022/2432758

[2]. Abdelmoneim, D., Porter, G. C., Coates, D. E., Duncan, W. J., Waddell, J. N., Hammer, N., & Li, K. C. (2022). The effect of low-processing temperature on the physicochemical and mechanical properties of bovine hydroxyapatite bone substitutes. *Materials*, 15(8), 2798.

https://doi.org/10.3390/ma15082798

[3]. Abdelmoneim, D., Porter, G., Duncan, W., Lim, K., Easingwood, R., Woodfield, T., & Coates, D. (2023). Three-dimensional evaluation of the cytotoxicity and antibacterial properties of alpha lipoic acid-capped silver nanoparticle constructs for oral applications. *Nanomaterials*, 13(4), 705.

https://doi.org/10.3390/nano13040705

[4]. Cotton, G. C., Gee, C., Jude, A., Duncan, W. J., Abdelmoneim, D., & Coates, D. E. (2019). Efficacy and safety of alpha lipoic acid-capped silver nanoparticles for oral applications. *RSC Advances*, 9(12), 6973-6985.

https://doi.org/10.1039/C9RA00613C

[5]. Inchingolo, F., Hazballa, D., Inchingolo, A. D., Malcangi, G., Marinelli, G., Mancini, A., & Dipalma, G. (2022). Innovative concepts and recent breakthrough for engineered graft and constructs for bone regeneration: A literature systematic review. *Materials*, 15(3), 1120.

https://doi.org/10.3390/ma15031120

[6]. Jin, J., Wu, Y., Liang, L., Wei, Y., Zheng, X., & Chen, Y. (2023). Altering sliver nanoparticles-induced inhibition to

bacterial denitrification via visible light by regulating silver transformation and adaptive mechanism under anaerobic conditions. *Chemical Engineering Journal*, 452, 139268.

https://doi.org/10.1016/j.cej.2022.139268

[7]. Lim, K. S., Klotz, B. J., Lindberg, G. C., Melchels, F. P., Hooper, G. J., Malda, J., & Woodfield, T. B. (2019). Visible light cross-linking of gelatin hydrogels offers an enhanced cell microenvironment with improved light penetration depth. *Macromolecular Bioscience,* 19(6), 1900098.

https://doi.org/10.1002/mabi.201900098

[8]. Martins, N., & Rodrigues, C. F. (2020). Biomaterial-related infections. *Journal of Clinical Medicine*, 9(3), 722.

https://doi.org/10.3390/jcm9030722

[9]. Mendes, C. R., Dilarri, G., Forsan, C. F., Sapata, V. D. M. R., Lopes, P. R. M., de Moraes, P. B., & Bidoia, E. D. (2022). Antibacterial action and target mechanisms of zinc oxide nanoparticles against bacterial pathogens. *Scientific Reports*, 12(1), 2658.

https://doi.org/10.1038/s41598-022-06657-y

[10]. Mukaratirwa-Muchanyereyi, N., Gusha, C., Mujuru, M., Guyo, U., & Nyoni, S. (2022). Synthesis of silver nanoparticles using plant extracts from Erythrina abyssinica aerial parts and assessment of their anti-bacterial and anti-oxidant activities. *Results in Chemistry*, 4, 100402.

https://doi.org/10.1016/j.rechem.2022.100402

[11]. Porter, G. C., Abdelmoneim, D., Li, K. C., Duncan, W. J., & Coates, D. E. (2022). The effect of low-temperature thermal processing on bovine hydroxyapatite bone substitutes, toward bone cell interaction and differentiation. *Materials*, 15(7), 2504.

https://doi.org/10.3390/ma15072504

[12]. Porter, G. C., Duncan, W. J., Jude, A., Abdelmoneim, D., Easingwood, R. A., & Coates, D. E. (2021). Endocytosed silver nanoparticles degrade in lysosomes to form secondary nanoparticle structures during expression of autophagy genes in osteogenic cells. *Nanomedicine: Nanotechnology, Biology and Medicine*, 33, 102355.

https://doi.org/10.1016/j.nano.2020.102355

[13]. Qing, T., Mahmood, M., Zheng, Y., Biris, A. S., Shi, L., & Casciano, D. A. (2018). A genomic characterization of the influence of silver nanoparticles on bone differentiation in MC3T3-E1 cells. *Journal of Applied Toxicology*, 38(2), 172-179.

https://doi.org/10.1002/jat.3528

[14]. Singh, P., & Mijakovic, I. (2022). Green synthesis and antibacterial applications of gold and silver nanoparticles from Ligustrum vulgare berries. *Scientific Reports*, 12(1), 7902.

https://doi.org/10.1038/s41598-022-11811-7

[15]. Wi, Y. M., & Patel, R. (2018). Understanding biofilms and novel approaches to the diagnosis, prevention, and treatment of medical device-associated infections. *Infectious Disease Clinics*, 32(4), 915-929.

https://doi.org/10.1016/j.idc.2018.06.009

[16]. Xu, Y., Zheng, B., He, J., Cui, Z., & Liu, Y. (2019). Silver nanoparticles promote osteogenic differentiation of human periodontal ligament fibroblasts by regulating the RhoA–TAZ axis. *Cell Biology International*, 43(8), 910-920. https://doi.org/10.1002/cbin.11180

ABOUT THE AUTHORS

Atheena Milagi Pandian is the Founder and Chief Executive Officer of Atheenapandian Private Limited, Tamil Nadu, India. He graduated in Biomedical Engineering in both undergraduation and postgraduation at Anna University (Government of Tamil Nadu) in Chennai, Tamil Nadu, India. He completed his Doctorate at the University of Tango in Thimphu, Bhutan. His research activities are mostly related to Healthcare, with particular interest in the fields of Medical Instrumentation and Prosthetics.

Rashika Murugan is the Chief Training Officer for Atheenapandian Private Limited, Tamil Nadu, India, and a Life Member of the Biomedical Engineering Society of India. She completed her Bachelor's degree in the field of Biomedical Engineering. Her research activities are based on Biosignals and Rehabilitation, and she has participated in various national and international conferences worldwide.

Mohammed Sahil S. serves as a Senior Biomedical Trainer and Head of Operations at the National and International Conferences for the Atheenapandian Organization in Tamil Nadu, India. He specializes in Biomedical Instrumentation, Rehabilitation Engineering, and Virtual Reality.